Cationic Europium Complexes for Visualizing Fluctuations in Mitochondrial ATP Levels in Living Cells

Romain Mailhot[a], Thomas Traviss-Pollard[a], Robert Pal[b] and Stephen J. Butler*[a]

Abstract: The ability to study cellular metabolism and enzymatic processes involving adenosine triphosphate (ATP) is impeded by the lack of imaging probes capable of signalling the concentration and distribution of intracellular ATP rapidly, with high sensitivity. We report here the first example of a luminescent lanthanide complex capable of visualizing changes in the concentration of ATP in the mitochondria of living cells. Four cationic europium(III) complexes [**Eu.1**–**4**]$^+$ have been synthesized and their binding capabilities towards nucleoside polyphosphate anions examined in aqueous solution at physiological pH. Complexes [**Eu.1**]$^+$ and [**Eu.3**]$^+$ bearing hydrogen bond donor groups in the pendant arms showed excellent discrimination between ATP, ADP and monophosphate species. Complex [**Eu.3**]$^+$ showed relatively strong binding to ATP (log K_a = 5.8), providing a rapid, long-lived luminescent signal that enabled its detection in a highly competitive aqueous medium containing biologically relevant concentrations of Mg^{2+}, ADP, GTP, UTP and human serum albumin. This Eu(III) complex responds linearly to ATP within the physiological concentration range (1–5 mM), and was used to continuously monitor the apyrase-catalyzed hydrolysis of ATP to ADP *in vitro*. We demonstrate that [**Eu.3**]$^+$ can permeate mammalian (NIH-3T3) cells efficiently and localize to the mitochondria selectively, permitting real-time visualization of elevated mitochondrial ATP levels following treatment with a broad spectrum kinase inhibitor, staurosporine, as well as depleted ATP levels upon treatment with potassium cyanide under glucose starvation conditions.

Introduction

Our understanding of cellular metabolism and a variety of biological processes involving adenosine triphosphate (ATP) is limited. Despite its importance, there is surprisingly few imaging probes capable of signalling the presence of ATP rapidly, reversibly and selectively under physiological conditions. We have addressed this challenge by creating a luminescent europium complex capable of imaging dynamic changes in the concentration of ATP in the mitochondria of living cells. ATP is the most abundant nucleoside polyphosphate (NPP) anion in cells and serves as the chemical energy source for most biological processes, including organelle transport, muscle contraction and maintenance of neuronal membrane potential.[1–3] The majority of ATP is generated by the mitochondria by oxidative phosphorylation. Numerous enzymes utilize ATP as a substrate, including ATPases, kinases, and RNA polymerases; thus ATP plays a key role in the regulation of protein and enzyme function. In order to study these dynamic processes, non-invasive imaging probes are needed that can signal ATP levels by modulation of luminescence, thereby providing spatial and temporal information with high sensitivity.

Current methods for monitoring the concentration of ATP in living cells are limited.ref The enzyme firefly luciferase can be expressed in cells to measure ATP levels indirectly, by catalyzing a chemiluminescent reaction between ATP and luciferin.[4] However, this method is irreversible and cannot be used to visualize changes in ATP levels that occur according to the metabolic demands of the cell.ref Additionally, luciferase consumes ATP, which prevents its accurate quantification.ref A few genetically encoded fluorescent biosensors have been developed to measure ATP successfully within specific cellular compartments.[5] However, biosensors encoded within cells require time consuming protein expression and maturation procedures and are intrinsically pH sensitive;ref small changes in intracellular pH (<0.1 units) have been shown to generate bias in the emission response, which can complicate interpretation of the observed signal.ref

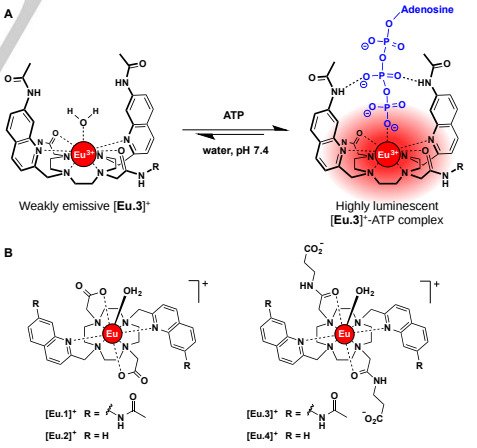

Figure 1. (A) Signalling mechanism and proposed binding mode between [**Eu.3**]$^+$ and ATP; (B) Structures of cationic Eu(III) complexes [**Eu.1**–**4**]$^+$.

[a] Mr. R. Mailhot, Mr. T. Traviss-Pollard and Dr. S. J. Butler
Department of Chemistry
Loughborough University
Epinal Way, Loughborough, LE11 3TU, UK
E-mail: s.j.butler@lboro.ac.uk
[b] Dr. R. Pal
Department of Chemistry
Durham University
South Road, Durham, DH1 3LE, UK

Supporting information for this article is given via a link at the end of the document.

An attractive alternative strategy involves the creation of discrete ATP-responsive synthetic receptors that exhibit intrinsic cellular uptake and localization behaviour.ref The majority of synthetic receptors for ATP comprise a fluorescent organic indicator linked to a positively charged recognition group, such as imidazolium or guanidinium units, or coordinated zinc(II) ions, which form strong electrostatic or metal-ligand interactions with the triphosphate fragment of ATP.[6] Only a few ATP-selective probes have been successfully applied to imaging ATP in living cells.[7a-d] Each of these probes emits a short-lived fluorescence signal, typically at wavelengths between 375 and 540 nm. Consequently, their signal overlaps with background autofluorescence arising from endogenous proteins, making intensity-based measurements problematic.ref In two cases, the detection range of the receptor is very low (0.1–10 μM),[7a, 7b] and the fluorescence response is saturated at ATP concentrations below those expected in cells (1–5 mM).[8] Chang and co-workers developed a probe capable of detecting ATP within the 2–10 mM range, in a viscous medium of glycerol/water (60:40).[7c] However, this probe is unable to respond to ATP in 100% aqueous solution at physiological pH, hence its utility in live-cell imaging is limited and dependent on variations in viscosity within the cell.

Importantly, during *in vitro* testing, anion affinity and selectivity are rarely assessed in a competitive ionic medium that resembles intracellular fluid.[7c] This is critical, because it defines the target concentration range and the nature and abundance of potentially interfering species, including other phosphoanions (e.g. ADP, AMP, GTP, HPO_4^{2-}), cations that bind strongly to ATP (e.g. Mg^{2+} and Ca^{2+} ions), and proteins, which can interact with the probe causing either quenching or enhancement of emission. The influence of such a competitive ionic environment on the probe's anion affinity and selectivity must be studied, to optimize its practical utility in live-cell imaging experiments.ref

In recent years, stable luminescent europium(III) and terbium(III) complexes have emerged as attractive tools for use in cellular imaging.cite selvin[9] Notably, a series of the brightest Eu(III) complexes have been developed as efficient cellular stains designed to localize preferentially in specific organelles.[10, 11] Stable Eu(III) and Tb(III) complexes offer significant advantages over conventional fluorescent organic dyes, including a large separation between the absorption and emission bands, long emission lifetimes (within the millisecond range) that enable complete removal of background autofluorescence by using time-resolved imaging techniques, and well-defined emission bands that permit ratiometric analysis. Certain Eu(III) and Tb(III) complexes have been shown to bind reversibly to anions in aqueous media, including bicarbonate,[12] fluoride,[13] lactate,[14] phosphate[15] and phosphorylated peptides[16]. Anion binding can be signalled by changes in the intensity ratio of two Ln(III) emission bands or by changes in emission lifetime of the complex.[17, 18] However, examples of Ln(III) complexes that bind to NPP anions such as ATP are rare.[19–21] Binding to ATP is usually weak and causes quenching of luminescence due to energy transfer to the nucleotide base[19, 21] or displacement of a coordinated sensitizing ligand from the Ln(III) ion (decomplexation).[15b, 22, 23] Probes that rely upon quenching of luminescence are less desirable for use in cellular imaging as other competitive quenching processes can generate the observed decrease in emission intensity.ref

In this work, we report a series of luminescent cationic Eu(III) complexes [**Eu.1–4**]$^+$ that bind reversibly and with differential affinities to NPP anions in aqueous solution at physiological pH (Figure 1). Each Eu(III) complex is based on a C_2-symmetric octadentate ligand bearing two coordinating quinoline groups that sensitize Eu(III) luminescence. Addition of ATP to complexes [**Eu.1**]$^+$ and [**Eu.3**]$^+$ results in rapid displacement of the coordinated water molecule, giving rise to dramatic enhancements in Eu(III) luminescence. Complex [**Eu.3**]$^+$ is very effective at binding to ATP in water at physiological pH, by means of a strong metal-ligand interaction, possibly strengthened by hydrogen bonds to the quinoline amide arms. [**Eu.3**]$^+$ can discriminate effectively between ATP and ADP in the presence of high concentrations of Mg^{2+} ions, permitting real-time analysis of the enzymatic hydrolysis of ATP to ADP *in vitro*. We demonstrate that [**Eu.3**]$^+$ can signal changes in the ratio of ATP/ADP in a simulated intracellular fluid containing biorelevant concentrations of several NPP anions including GTP and UTP, as well as Mg^{2+} ions and protein. [**Eu.3**]$^+$ was shown to permeate NIH-3T3 cells efficiently and localize selectively to the mitochondria, providing a strong luminescent signal that can report on dynamic changes in mitochondrial ATP levels within living cells. This new class of Eu(III) complexes offers a number of improvements in performance compared to existing probes for ATP, including a long-lived luminescence signal that is sensitive to ATP levels within the physiological range (1–5 mM), with minimal interference from biomolecule autofluorescence or changes in cellular pH. In addition, [**Eu.3**]$^+$ possesses a distinctive subcellular localization profile that allows ATP levels to be monitored within a specific region of the cell.

Results and Discussion

Complex Design and Synthesis. Each Eu(III) complex contains two coordinating quinoline groups that act as efficient sensitizers of Eu(III) emission.ref Complexes [**Eu.1**]$^+$ and [**Eu.2**]$^+$ were synthesised previously[13a] and possess two negatively charged carboxylate groups that coordinate to the Eu(III) ion, whereas complexes [**Eu.3**]$^+$ and [**Eu.4**]$^+$ possess two neutral carbonyl amide donor groups, functionalized with terminal carboxylate moieties to increase water solubility. The carbonyl amide groups in [**Eu.3**]$^+$ and [**Eu.4**]$^+$ were expected to increase the electropositive nature of the Eu(III) metal compared to [**Eu.1**]$^+$ and [**Eu.2**]$^+$, thus strengthening the electrostatic interaction between the Eu(III) ion and negatively charged NPP anions in aqueous solution. Additionally, it was envisaged that the increased local positive charge of [**Eu.3**]$^+$ and [**Eu.4**]$^+$, together with the amphipathic nature of the surrounding ligands, would facilitate cellular uptake of the Eu(III) complexes, and potentially promote selective localization to the negatively charged inner membrane of the mitochondria.[11, 7a]

Complexes [**Eu.1**]$^+$ and [**Eu.3**]$^+$ possess hydrogen-bond donor (amide) groups at the 7-position of the coordinated quinoline chromophores. We envisaged that NPP anions such as ATP

would coordinate to the Eu(III) ion *via* the terminal phosphate group, enabling the adjacent phosphate group to engage in hydrogen bonding interactions with quinoline amide N–H groups (Figure 1B), thereby enhancing selectivity over monophosphate species. Indeed, we have shown recently that the cooperative use of metal-ligand interactions in combination with hydrogen bonding can provide excellent selectivity for nucleoside polyphosphate anions over monophosphate anions (e.g. AMP, cAMP, HPO_4^{2-}, phosphorylated amino acids), where no such hydrogen-bonding interactions can occur.[24, 25] To demonstrate the function of the hydrogen bond-donor groups in the ATP recognition process, we prepared two control complexes, [**Eu.2**]$^+$ and [**Eu.4**]$^+$, which lack quinoline amide groups.

Details of the synthesis and characterization of complexes [**Eu.3**]$^+$ and [**Eu.4**]$^+$ are provided in the supporting information (Fig. S1–S3 for synthetic schemes). Briefly, a cyclen derivative bearing two *trans*-related secondary amines was reacted with an appropriately functionalized 2-methylquinoline mesylate ester or 2-(chloromethyl)quinoline in the presence of K_2CO_3, to give the protected macrocyclic ligand. The terminal ethyl ester protecting groups of the two carbonyl amide arms were hydrolyzed using 0.45 M NaOH solution. Subsequent addition of one equivalent of $EuCl_3$ in a mixture of water/methanol at pH 7–8 gave the water soluble Eu(III) complexes [**Eu.3**]$^+$ and [**Eu.4**]$^+$, after purification by preparative reverse-phase HPLC.

Table 1. Selected photophysical data for complexes [**Eu.1–4**]$^+$, measured in 10 mM HEPES, pH 7.0, 25°C.

Complex	λ_{max}/ nm	ε/M^{-1}cm^{-1}	ϕ_{em}/%[a]	τ_{H2O}/ms	τ_{D2O}/ms
[**Eu.1**]$^+$	332	0.00125	7.0	0.49	1.38
[**Eu.2**]$^+$	318	0.00118	23	0.51	1.37
[**Eu.3**]$^+$	330	0.00077	6.5	0.56	1.22
[**Eu.4**]$^+$	318	0.00210	18	0.60	1.29

[a] Quantum yields were measured using $[Ru(bpy)_3]Cl_2$ in water as a standard (ϕ_{em} = 0.028).[1] Errors in quantum yields and lifetimes are ±15%; [b] Values of hydration state, *q* (±20%) were derived using literature methods.[26]

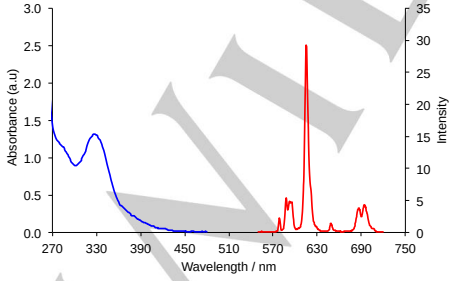

Figure 2. Absorption (*blue*) and emission (*red*) spectra of [**Eu.3**]$^+$, recorded in buffered aqueous solution (10 mM HEPES) at pH 7.0. λ_{exc} = 330 nm, 25°C.

Table 1 shows selected photophysical data for [**Eu.1–4**]$^+$. The UV-Vis absorption spectra of [**Eu.1**]$^+$ and [**Eu.3**]$^+$ are similar and comprise of a broad band centred at 332 nm and 330 nm respectively, tailing out to 370 nm, whereas [**Eu.2**]$^+$ and [**Eu.4**]$^+$ each feature two narrow bands with maxima at 303 and 318 nm (Fig. S4-S7). The emission spectra for each complex in aqueous buffer (10 mM HEPES, pH 7.4) was well separated from the absorption spectra, as illustrated by [**Eu.3**]$^+$ in Figure 2. The emission spectra of [**Eu.1**]$^+$, [**Eu.2**]$^+$ and [**Eu.4**]$^+$ showed similarities, displaying at least three components in the ΔJ = 1 (585–605 nm) band, and two distinguishable components within the ΔJ = 2 (605–630 nm) band, consistent with each complex adopting a structure of low symmetry in water (Fig. S8). For [**Eu.3**]$^+$, a rather different emission spectrum was obtained, characterised by an intense ΔJ = 2 band around 605–630 nm in the red region of the visible spectrum (Figure 2). Emission quantum yields were in the range 7–23% and emission lifetimes in H_2O were measured to be approximately 0.5 ms, and at least 50% larger in D_2O. The number of coordinated water molecules, *q*, was determined to be one for each Eu(III) complex.[26] These data suggested that complexes [**Eu.1**]$^+$ and [**Eu.3**]$^+$ were most suited for use in live-cell imaging experiments, due to their high water solubility, long-lived luminescence, large ligand-induced Stokes' shifts and sufficiently long excitation wavelengths of over 350 nm, thereby matching the optics of standard fluorescence microscopes.

Anion Binding Studies at Physiological pH. The Eu(III) emission spectra of [**Eu.1–4**]$^+$ was recorded in pH 7.0 (10 mM HEPES) in the presence of a range of anions (1 mM) (Fig. S9–S12). Addition of 1 mM ATP to [**Eu.1**]$^+$ or [**Eu.3**]$^+$ resulted in an immediate 10-fold enhancement in Eu(III) emission intensity of the hypersensitive ΔJ = 2 band (605–630 nm), whereas adding ADP induced a 14-fold increase in emission intensity. AMP and HPO_4^{2-} induced a much smaller (approximately 2-fold) increase in emission intensity while other monophosphate anions including cyclic AMP and phosphorylated amino acids (pSer, pThr, pTyr) induced negligible spectral responses, as did chloride, sulphate, lactate, acetate, glutathione, Na^+, K^+, Zn^{2+}, Mg^{2+} and Ca^{2+} ions. The guanosine phosphate anions, GTP, GDP and GMP induced similar spectral responses to those observed for ATP, ADP and AMP respectively. The only other anions tested that induced a significant spectral response were citrate and bicarbonate, which caused a maximum 4-fold and 5-fold increase in Eu(III) emission intensity, respectively. Control complexes [**Eu.2**]$^+$ and [**Eu.4**]$^+$, which lacked quinoline amide groups, showed a much lower level of discrimination between NPP anions: a maximum 3-fold enhancement in intensity of the ΔJ = 2 emission band was observed in the presence of 1 mM ATP, ADP and AMP.

The emission intensity of [**Eu.3**]$^+$ was found to be particularly sensitive to ATP concentration. Figure 3 shows the increase in emission spectra of [**Eu.3**]$^+$ in the presence of increasing ATP levels (0–180 µM), revealing a dramatic 17-fold enhancement in intensity at 614 nm within the ΔJ = 2 band. Notably, the emission spectral shape of [**Eu.3**]$^+$ did not change significantly, suggesting that only minor changes in coordination geometry of [**Eu.3**]$^+$ occur upon binding to ATP. Emission lifetimes of [**Eu.3**]$^+$ measured in

Commented [SB1]: add reference here: K. Nakamaru, Bull, Chem. Soc. Jpn., 1982, 55, 2697-2705.

H_2O and D_2O in the absence and presence of ATP were consistent with a hydration state, *q*, of 0.8 (±20%) and zero, respectively (Table S1), establishing that ATP displaces the coordinated water molecule from the Eu(III) metal, accompanied by a pronounced increase in luminescence.

Table 2. Apparent binding constants (log K_a) determined for [**Eu.1–4**]$^+$ and different anionic species in aqueous solution (10 mM HEPES, pH 7.0, 25°C).

Anion	Log K_a [a]			
	[**Eu.1**]$^+$	[**Eu.2**]$^+$	[**Eu.3**]$^+$	[**Eu.4**]$^+$
ATP	4.4	3.0	5.8	3.8
ADP	4.6	3.3	5.7	3.8
AMP	3.4	3.3	4.8	3.5
PPi	3.5	2.4	4.7	3.4
GTP	4.4	n/d	5.3	n/d
GDP	4.6	n/d	5.2	n/d
GMP	3.4	n/d	3.9	n/d
UTP	3.6	n/d	4.9	n/d
UDP	4.2	n/d	5.4	n/d
UMP	2.7	n/d	4.3	n/d
HPO_4^{2-}	n.d	n/d	2.7	n/d
HCO_3^-	3.0[b]	n/d	3.0	n/d

[a] Each value represents the average of at least two duplicate titration experiments. Errors in measurements were ± 0.1 with the statistical error associated with the fit of the data <0.05. n/d = not determined. [b] Values determined previously in 25 mM HEPESunder the same conditions.

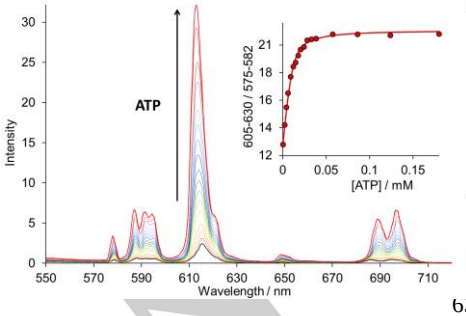

Figure 3. Change in emission spectra of [**Eu.3**]$^+$ (5 μM) as a function of added ATP (0–180 μM) in aqueous solution at pH 7.0; (Inset) Binding isotherm and fit to the experimental data, for log K_a = 5.8 (± 0.1). Conditions: 10 mM HEPES buffer, pH 7.0, λ_{exc} = 330 nm, 25°C.

Apparent binding constants were determined for complexes [**Eu.1–4**]$^+$ and a range of NPP anions by following the change in the intensity ratio of the $\Delta J = 2/\Delta J = 1$ (605–630/580–600 nm) emission bands as a function of anion concentration, followed by a non-linear, least squares curve-fitting procedure based on a 1:1 binding model (Table 2 and Fig. S13–S43).‡ [**Eu.3**]$^+$ showed the strongest binding to ATP and ADP (log K_a = 5.8 and 5.7 respectively), approximately 10 times stronger than to AMP and pyrophosphate (PPi), and 100 times stronger than to HPO_4^{2-} and HCO_3^- (log K_a = 2.7 and 3.0 respectively). [**Eu.1**]$^+$ showed a similar level of selectivity between ATP, ADP, AMP and PPi, however the affinity for each anion was approximately one order of magnitude lower, and HPO_4^{2-} showed no significant binding interaction. The higher affinity of [**Eu.3**]$^+$ for ATP compared to [**Eu.1**]$^+$ can be attributed to replacement of the negatively charged carboxylate donors in [**Eu.1**]$^+$ with neutral carbonyl amide donors in [**Eu.3**]$^+$, increasing the electropositive nature of the Eu(III) ion, causing it to interact more strongly with ATP.

The selectivity of [**Eu.1**]$^+$ and [**Eu.3**]$^+$ for ATP and ADP over monophosphate anions can be attributed to increased Coulombic attraction as well as stabilizing hydrogen bonding interactions between the coordinated phosphate fragment of ATP (and ADP) and the amide N-H groups of the quinoline chromophores (Figure 1). In support of this, [**Eu.2**]$^+$ and [**Eu.4**]$^+$, which lack amide groups, showed significantly lower affinities and essentially no selectivity between ATP, ADP, AMP and PPi. Hence, binding of NPP anions to [**Eu.1**]$^+$ and [**Eu.3**]$^+$ is not governed solely by favourable electrostatic interactions, but involves additional stabilization *via* hydrogen bonding that leads to enhanced selectivity towards ATP and ADP over monophosphate species.

Complexes [**Eu.1**]$^+$ and [**Eu.3**]$^+$ were found to bind to the guanosine and uridine phosphate anions with a similar level of selectivity to that determined for the adenosine phosphate series; the general order of affinity was found to be NTP≈NDP>NMP. The nucleoside moiety appears to contribute towards anion binding, as both [**Eu.1**]$^+$ and [**Eu.3**]$^+$ bind to NMP anions but show very weak affinity to HPO_4^{2-}, and bind to nucleoside diphosphate anions 10 times more strongly than to pyrophosphate. Due to the lack of binding selectivity and small spectral responses exhibited for [**Eu.2**]$^+$ and [**Eu.4**]$^+$ with adenosine phosphate anions, affinity constants for other NPP anions were not determined.

Evidence for 1:1 binding between [**Eu.3**]$^+$ and ATP or GTP was provided by high resolution (ESI) mass spectrometric data, which showed intense signals at m/z = 741.6588 and 749.6564, corresponding to the doubly charged species [**Eu.3**+ATP+5H]$^{2+}$ and [**Eu.3**+GTP+5H]$^{2+}$ respectively (Fig. S44 and S45).§ Mass spectral evidence for the formation of stable ternary adducts of [**Eu.1**]$^+$ and ATP or ADP was reported previously.[24]

Effect of Mg^{2+} ions in solution. The majority of intracellular ATP exists in the form Mg-ATP^{2-}.[27] Therefore, a cellular imaging probe for ATP should ideally be able to bind to the Mg-ATP^{2-} complex. Indeed, enzymes that require ATP as a substrate, such as ATPases and kinases, utilize Mg^{2+} ions to provide additional stabilization of the ATP-enzyme complex.[28] The binding interaction between Mg^{2+} ions and ATP in water at physiological pH is approximately 50 times stronger than the interaction with

ADP, with log K_a (Mg-ATP) = 4.2 and log K_a (Mg-ADP) = 3.6.[29] The presence of Mg^{2+} ions in aqueous solution was expected to influence the ability of complexes [**Eu.1**]$^+$ and [**Eu.3**]$^+$ to discriminate between ATP and ADP. Indeed, previously reported synthetic receptors have shown limited discrimination between ATP and ADP at enzyme relevant concentrations of Mg^{2+} ions.[20, 30] We showed recently that [**Eu.1**]$^+$ can discriminate

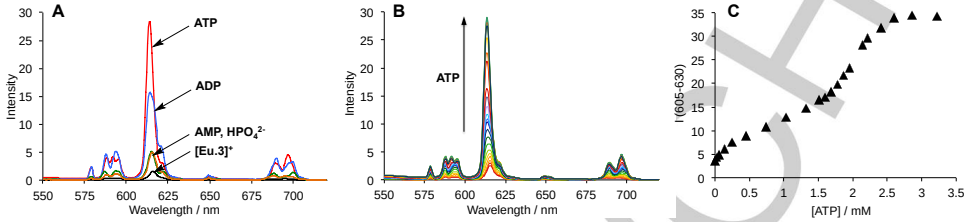

Figure 4. Selective spectral response of [**Eu.3**]$^+$ for ATP in the presence of Mg^{2+} ions. (A) Change in emission spectra of [**Eu.3**]$^+$ (5 μM) in the presence of 2 mM ATP, ADP, AMP and HPO_4^{2-} in a fixed background of 5 mM $MgCl_2$; (B) Variation in emission spectra of [**Eu.3**]$^+$ upon addition of ATP (0–3 mM) in a fixed background of 5 mM $MgCl_2$; (C) Increase in intensity of the ΔJ = 2 band (605–630 nm) of [**Eu.3**]$^+$ as a function of ATP concentration. Conditions: 10 mM HEPES buffer, pH 7.4, λ_{exc} = 330 nm, 25°C.

effectively between ATP and ADP in a buffered aqueous solution containing 3 mM Mg^{2+} ions: adding 1 mM ADP caused an 8-fold increase in overall Eu(III) emission intensity compared to a much smaller 2.5-fold intensity increase in the presence of 1 mM ATP.[24] Excellent discrimination between ATP and ADP was attributed to the slightly higher affinity of [**Eu.1**]$^+$ for ADP (Table 1) as well as the higher competition between Mg^{2+} and ATP compared to ADP. This allowed the change in the ratio of ATP/ADP to be dynamically followed during the course of a kinase-catalyzed phosphorylation reaction.

Complex [**Eu.3**]$^+$ showed a different discriminatory behaviour between ATP and ADP in the presence of Mg^{2+} ions. Figure 4A shows the emission spectral response of [**Eu.3**]$^+$ in the presence of 2 mM ATP, ADP, AMP and HPO_4^{2-} in a fixed background of 5 mM Mg^{2+} ions. Adding 2 mM ATP resulted in a substantial 24-fold enhancement in intensity of the ΔJ = 2 emission band, whereas ADP caused a smaller 13-fold increase in luminescence. Only minor changes in emission spectra took place in the presence of AMP and HPO_4^{2-}. Titrations of ADP and AMP into an aqueous solution containing [**Eu.3**]$^+$ and 5 mM Mg^{2+} ions resulted in standard hyperbolic curves that were fitted to a 1:1 binding model (Fig. S50 and S51). Apparent association constants were determined to be log K_a = 4.6 and 3.8 for ADP and AMP respectively, approximately 1 order of magnitude lower than those determined in the absence of $MgCl_2$.

A titration of ATP in a fixed background of 5 mM Mg^{2+} ions generated an isotherm consistent with the occurrence of two distinct emissive species (Figure 4C). Incremental addition of 0–1.5 mM ATP gave rise to a 4-fold increase in emission intensity of the ΔJ = 2 band, and subsequent addition of 1.5–3.0 mM ATP induced a further 3-fold enhancement in Eu(III) emission, with no discernable change in spectral form. This can be ascribed to the formation of two discrete ternary adducts, each exhibiting a similar coordination environment at the Eu(III) ion. It is hypothesized that [**Eu.3**]$^+$ binds to either ATP or the Mg-ATP^{2-} complex; with the binding geometry between [**Eu.3**]$^+$ and Mg-ATP^{2-} being similar to that of ATP, and stabilization of the negatively charged triphosphate fragment provided by the Mg^{2+} ion (Figure 1B). During the ATP titration, the concentration of Mg-ATP^{2-} increases, leading to the formation of a highly emissive ternary complex. High resolution mass spectrometric data supported binding of [**Eu.3**]$^+$ to Mg-ATP^{2-}, giving an intense signal at 752.6439 corresponding to the doubly charged species [**Eu.3**+ATP+Mg+3H]$^{2+}$, which was in excellent agreement with the calculated isotopic distribution (Fig. S46). A titration of ATP in a fixed background of NaCl (100 mM) revealed a classic isotherm for a simple 1:1 binding system, with an apparent binding constant of log K_a = 5.0 (Fig. S52). This confirms that the changes in emission spectra of [**Eu.3**]$^+$ in the presence of Mg^{2+} ions cannot be simply a result of the additional ionic strength of the medium, rather it is the specific interactions between Mg^{2+}, ATP and the Eu(III) complex that modulates the equilibrium speciation and resulting emission response.

Monitoring ATPase Activity in Real-Time. Having established that [**Eu.3**]$^+$ exhibits a selective spectral response towards ATP over ADP in a background of 5 mM Mg^{2+} ions, we demonstrated the ability of the Eu(III) complex to monitor the apyrase-catalyzed hydrolysis of ATP in real-time. Apyrase is an enzyme that catalyzes the conversion of ATP into ADP, releasing energy in the process. To a buffered aqueous solution (10 mM HEPES, pH 7.0) containing [**Eu.3**]$^+$ (5 μM) and ATP (2 mM) was added different amounts of apyrase (80–160 mU, ATP/ADP selectivity ratio, 10:1). The conversion of ATP to ADP and HPO_4^{2-} caused a time-dependent decrease in emission intensity of the ΔJ = 2 band centred at 614 nm and a smaller increase in intensity at 594 nm within the ΔJ = 1 band (Figure 5A). Plots of the emission intensity ratio at 614/594 nm as a function of time revealed that the rate of ATP hydrolysis was directly proportional to the amount of enzyme added (Figure 5B). The background reaction in the absence of enzyme showed essentially no change in emission intensity during the time frame of the experiment. The ratiometric changes in emission intensity observed during the enzyme reaction were in good agreement with those obtained in a simulated ATPase

reaction, in which the ratio of ATP/ADP was varied systematically (Figure 5D).

Given that [**Eu.3**]$^+$ binds strongly to ATP, the possibility that the probe lowers the effective concentration of ATP must be considered, as this would influence the rate of reaction. However, anion binding to [**Eu.3**]$^+$ is fast and reversible, and due to the highly sensitive nature of the luminescence response, the amount of [**Eu.3**]$^+$ required to monitor the ATPase assay is much lower (5 μM) compared to the concentration of ATP (2 mM). This ensures that the rate of ATP hydrolysis is not perturbed by the presence of [**Eu.3**]$^+$.[31]

Figure 5C shows the linear decrease in emission intensity ratio at 614/594 nm during the initial stages (0–9 minutes) of each enzyme reaction. Reducing the amount of enzyme from 160 mU to 80 mU resulted in a decrease in the initial rate of ATP hydrolysis by a factor of two. Thus, [**Eu.3**]$^+$ is able to directly and continuously monitor ATPase activity by providing an instantaneous and ratiometric luminescent signal, without the need to chemically modify the enzyme or its substrate.

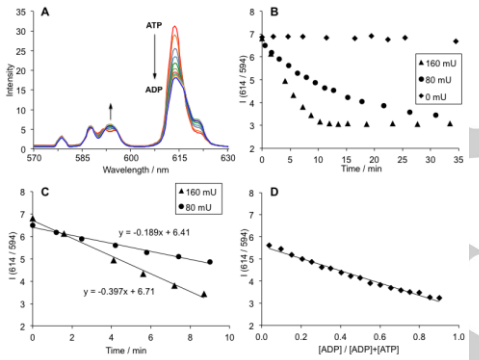

Figure 5. Continuous monitoring of apyrase catalyzed hydrolysis of ATP. (A) Change in emission spectra of [**Eu.3**]$^+$ (570–630 nm) during the apyrase (80 mU) catalyzed hydrolysis of ATP to ADP; (B) Time-trace plots showing the decrease in emission intensity ratio at 614/954 nm in the presence of different amounts of apyrase (0, 80 or 160 mU); (C) Linear change in emission intensity of [**Eu.3**]$^+$ during the initial stages of the enzyme reaction; (D) Plot of the emission intensity ratio at 614/594 nm versus mole fraction of ADP, in the absence of apyrase (total nucleotide, [ATP]+[ADP], is constant at 2 mM). Conditions: 10 mM HEPES, pH 7.0, [**Eu.3**]$^+$ (5 μM), apyrase (80 or 160 mU, ATP (2 mM). λ_{exc}= 330 nm, 25°C.

Evaluating Affinity to Protein. Encouraged by the ability [**Eu.3**]$^+$ to monitor the enzymatic conversion of ATP to ADP in real-time, we wished to evaluate the ability of [**Eu.3**]$^+$ monitor fluctuations in ATP levels in living mammalian cells. A cellular imaging probe for ATP must be able to operate in the presence of proteins. Emissive metal coordination complexes are known to interact non-covalently with proteins, often causing quenching or enhancement of emission.[32] We measured the affinity of complexes [**Eu.1**]$^+$ and [**Eu.3**]$^+$ for human serum albumin (HSA), the most abundant protein in human blood plasma. Addition of HSA (0–0.4 mM) to [**Eu.1**]$^+$ at pH 7.0 resulted in a 3.5 fold increase in overall Eu(III) emission intensity and distinctive changes in spectral form (Figure 6A). A plot of the intensity ratio of the Δ*J* = 2 / Δ*J* = 1 emission bands *versus* HSA concentration allowed an estimation of the association constant, log K_a = 4.8 (K_d = 16 μM) (Fig. S53). Luminescence lifetimes for the protein bound species in H_2O and D_2O were found to be 0.92 and 1.73 ms respectively,

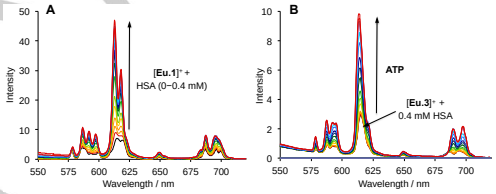

corresponding to a hydration state, *q* = 0. Thus, binding of [**Eu.1**]$^+$ to HSA involves displacement of the bound water molecule, possibly by coordination of an aspartate or glutamate residue of HSA.

In sharp contrast, incremental addition of HSA to [**Eu.3**]$^+$ caused a minor (10%) increase in Eu(III) emission intensity and no change in spectral form (Fig. S54). Analysis of the luminescence lifetimes of [**Eu.3**]$^+$ in the presence of HSA in H_2O and D_2O suggested displacement of the bound water molecule. A lower apparent binding affinity was estimated between [**Eu.3**]$^+$ and H SA (log K_a = 3.2, or K_d = XX μM), which is approximately 2.5 orders of magnitude lower than the binding constant determined for this complex and ATP, under the same conditions. The minimal interaction observed between [**Eu.3**]$^+$ and HSA could be tentatively attributed to the presence of two ancillary carboxylate groups in the macrocyclic ligand, which could minimize the occurrence of hydrophobic interactions between the Eu(III) complex and the protein. Gratifyingly, addition of increasing amounts of ATP (0–0.5 mM) to [**Eu.3**]$^+$ in a fixed background of 0.4 mM HSA gave rise to a measurable 3-fold increase in emission intensity of the Δ*J* = 2 band (Figure 6B), consistent with competitive displacement of the bound protein from [**Eu.3**]$^+$, upon binding to ATP. The apparent binding constant was estimated to be log K_a = 4.0 (Figure S55), approximately two orders of magnitude lower than that determined between [**Eu.3**]$^+$ and ATP in the absence of protein. Conversely, [**Eu.1**]$^+$ was unable to signal the presence of ATP under the same conditions.

ATP Recognition in Simulated Intracellular Fluid. The above competition experiments, involving biologically relevant amounts of protein and Mg^{2+} ions, encouraged us to examine the ability of

[**Eu.3**]$^+$ to detect ATP in an aqueous medium that mimics the complex ionic environment within cells. In a healthy cell, the most abundant NPP anion is ATP, which is estimated to be present in concentrations between 1–5 mM (average 3 mM).[8] The majority of ATP is generated by the mitochondria by oxidative phosphorylation. Importantly, ADP is maintained at a significantly lower concentration (50–200 μM), the majority of which is bound strongly to protein, such that the ATP/ADP ratio ranges between 5 and 100.[33] This ATP/ADP ratio acts as a critical modulator of a variety of cellular events. Other NPP anions including GTP, UTP and CTP are estimated to be present in concentrations 5-fold lower than that of ATP. An intracellular probe must be able to respond selectively to ATP under these conditions.

Figure 6. Differential responses of [**Eu.1**]$^+$ and [**Eu.3**]$^+$ to human serum albumin. (A) Change in emission spectra of [**Eu.1**]$^+$ in the presence of increasing amounts of HSA (0–0.4 mM); (B) Increase in emission spectra of [**Eu.3**]$^+$ upon titration of ATP (0–0.5 mM) in a fixed background of 0.4 mM HSA. Conditions: HEPES buffer (10 mM, pH 7.0), λ_{exc} = 330 nm, 25°C.

Using the above concentrations of NPP anions, we prepared a simulated intracellular fluid based on a modified Krebs saline solution, which is commonly used in cell and tissue culture experiments. The solution contains ADP (0.1 mM), GTP (0.5 mM) and UTP (0.5 mM), NaH_2PO_4 (0.9 mM), PPi (0.05 mM), KCl (110 mM), NaCl (10 mM), $CaCl_2$ (2.5 mM), $MgCl_2$ (8 mM), Na_2SO_4 (0.5 mM), sodium lactate (2.3 mM), sodium citrate (0.13 mM), glutathione (3 mM) and HSA (0.4 mM), buffered at pH 7.4 using 10 mM HEPES. Under these conditions, incremental addition of 0–6 mM ATP to [**Eu.3**]$^+$ (50 μM) resulted in a reproducible 55% enhancement in emission intensity of the ΔJ = 2 band centred at 614 nm (Figure 7). Crucially, the increase in Eu(III) emission intensity was approximately linear over a biologically relevant ATP concentration range of 0.3 to 8.0 mM, corresponding to an increase in the ATP/ADP ratio from 3 to 80 (Figure 7, inset). These competition experiments strongly indicated that [**Eu.3**]$^+$ could be used to signal changes in the ATP/ADP ratio in *cellulo*, allowing a range of biological processes to be followed in real-time.

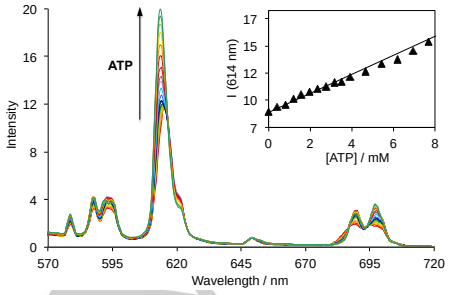

Figure 7. Detection of ATP in a simulated intracellular fluid. Change in emission spectra of [**Eu.3**]$^+$ (50 μM) upon titration of ATP over the physiological concentration range (0–8 mM); (Inset) Linear increase in Eu(III) emission intensity at 614 nm as a function of added ATP. Conditions: HEPES buffer (10 mM, pH 7.4), ADP (0.1 mM), GTP (0.5 mM), UTP (0.5 mM), $Na_4P_2O_7$ (0.05 mM), Na_2HPO_4 (0.9 mM), NaCl (10 mM), KCl (110 mM), $CaCl_2$ (2.5 mM), $MgCl_2$ (8 mM), Na_2SO_4 (0.5 mM), sodium lactate (2.3 mm), sodium citrate (0.13 mM), glutathione (3 mM), HSA (0.4 mM). λ_{exc} = 330 nm, 25°C.

Before undertaking cellular imaging studies, the pH dependence of the emission response of [**Eu.3**]$^+$ in the presence of 2 mM ATP was assessed. The emission intensity and spectral form was essentially unchanged between pH 6.4 and 8.6 (Fig. S56), suggesting that the luminescence signal should not be affected by pH fluctuations around normal mitochondrial or cytoplasmic pH, estimated to be near 7.3 and 8.0, respectively.[34] This is significant, as previous reports of ATP-selective imaging probes have been shown to be sensitive to small changes in intracellular pH.[5, 7c]

Imaging Mitochondrial ATP In Living Cells

Cellular Uptake and Localization Studies. The cellular uptake behaviour of [**Eu.3**]$^+$ was examined in NIH-3T3 cells using fluorescence and laser scanning confocal microscopy (LSCM).[35] Incubation of [**Eu.3**]$^+$ (50 μM) in NIH-3T3 cells for 2 hours resulted in uptake of the Eu(III) complex and predominant localization to the mitochondria (λ_{exc} 355 nm, λ_{em} 605–720 nm), verified by co-localization studies using MitoTracker Green (λ_{exc} 488 nm, λ_{em} 500–530 nm, Pearson's correlation coefficient, P = 0.91) (Figure 8). The preferential distribution of [**Eu.3**]$^+$ in the mitochondria could be tentatively attributed to the overall positive charge of the Eu(III) complex and the amphipathic nature of the macrocyclic ligand.[11] Imaging was possible over extended time periods (up to 8 hours), during which time the brightness of the observed images did not vary significantly (±10%) and the cells appeared to be healthy and proliferating (see supporting information for analysis of probe brightness within cells).

Cytotoxicity and vitality studies were undertaken for [**Eu.3**]$^+$ at 24 hours using image cytometry assays, involving DAPI and Acridine Orange stains, which revealed an IC_{50} value of greater than 200 μM. Considering that the incubation concentration of [**Eu.3**]$^+$ is four times lower than this value, it can be assumed that the Eu(III) complex is essentially non-toxic during the time frame of the imaging experiments. Analysis of ICP-MS data showed that for 4 × 10^6 NIH-3T3 cells incubated with [**Eu.3**]$^+$ (50 μM) for 2 hours, a given cell contained 69 μM (±5%) of Eu(III) metal, consistent with the accumulation of [**Eu.3**]$^+$ within the mitochondria during the incubation period.

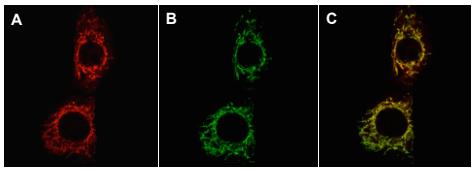

Figure 8. LSCM images showing mitochondrial localization of the Eu(III) complex. (A) Localization of [**Eu.3**]$^+$ (50 μM) in the mitochondria of NIH-3T3 cells

(λ_{exc} 355 nm, λ_{em} 605–720 nm); (B) MitoTracker Green (λ_{exc} 488 nm, λ_{em} 500–530 nm); (C) RGB merged image verifying co-localization (P = 0.91).

Imaging elevated mitochondrial ATP levels. We evaluated the ability of [**Eu.3**]$^+$ to visualize changes in the concentration of ATP in NIH-3T3 cells upon treatment with staurosporine, a broad-spectrum inhibitor of kinase activity that eventually induces cell apoptosis. Figure 9A shows time-lapsed images of cells stained with [**Eu.3**]$^+$ (50 μM) before (0 min) and after treatment with staurosporine (10 nM). The images revealed a gradual increase in the observed emission intensity (λ_{em} 605–720 nm) in the mitochondria over a 90-minute period. At 60 minutes post-staurosporine treatment, the Eu(III) emission intensity had increased by approximately 65%, after which time the observed signal reached a plateau (Figure 9B). No obvious signs of cell apoptosis were evident during the time scale of the experiment, and the Eu(III) complex remained localized to the mitochondria. As a control, cells incubated with [**Eu.3**]$^+$ without the addition of staurosporine were examined, revealing less than 10% variation in the Eu(III) emission intensity over the same time period (Fig. S57). ICP-MS studies of cells incubated with [**Eu.3**]$^+$ and staurosporine for 2 hours revealed essentially no change in the concentration of accumulated Eu(III) metal, compared to cells grown in the absence of the kinase inhibitor. Therefore, treatment with staurosporine does not appear to perturb cellular uptake or efflux of the Eu(III) complex from cells.

These imaging experiments indicate that the

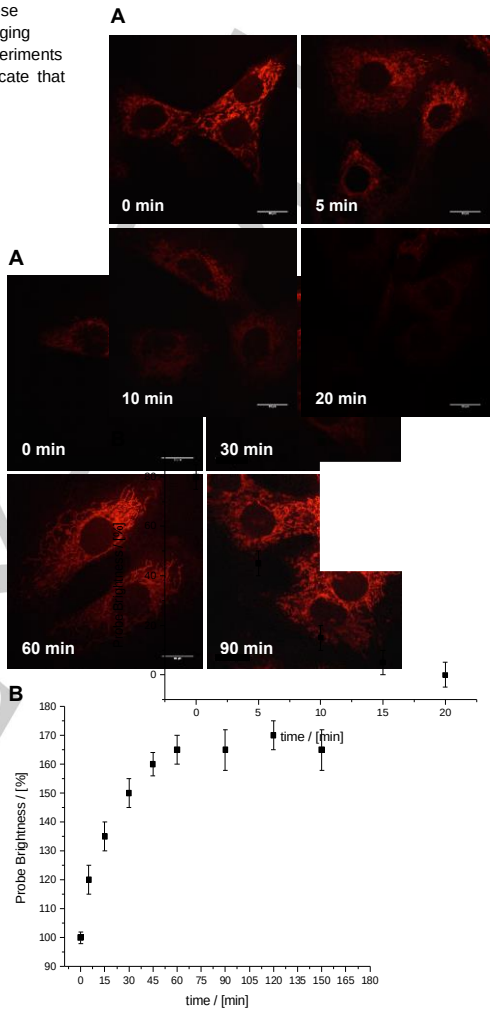

concentration of ATP in the mitochondrial region gradually increased during the preapoptotic period (150 min) following treatment with staurosporine. The mitochondria remained intact during this time, suggesting that mitochondrial functional integrity is important during the early stages of apoptosis. This is consistent with the notion that apoptosis is an energy requiring process; the concentration of mitochondrial ATP increases to supply chemical energy for a variety of intracellular processes, such as enzymatic hydrolysis of macromolecules.

Figure 9. Real-time monitoring of elevated levels of ATP in mitochondria. (A) Time-lapsed LSCM images of NIH-3T3 cells stained with [**Eu.3**]$^+$ (50 μM, λ_{exc} 355 nm, λ_{em} 605–720 nm) before (0 min) and after treatment with staurosporine (10 nM), a potent inhibitor of protein kinases; (B) Time-dependent increase in emission intensity (605–720 nm) of cells stained with [**Eu.3**]$^+$ following treatment with staurosporine (10 nM).

Figure 10. Real-time monitoring of depleted mitochondrial ATP levels. (A) Time-lapsed LSCM images of NIH-3T3 cells stained with [**Eu.3**]$^+$ (50 μM, λ_{exc} 355 nm, λ_{em} 605–720 nm) under glucose starvation conditions, before (0 min) and after treatment with KCN (0.1 mM), an inhibitor of oxidative phosphorylation; (B) Time dependent decrease in emission intensity of cells stained with [**Eu.3**]$^+$ following treatment with KCN (0.1 mM).

Monitoring depleted ATP levels in living cells. Next, the change in mitochondrial ATP levels was monitored after treatment of cells with potassium cyanide, an inhibitor of oxidative phosphorylation. Initially, NIH-3T3 cells were incubated with [**Eu.3**]$^+$ in a glucose-free growth medium, in order to inhibit ATP production *via* glycolysis. Under these conditions, a 20% decrease in emission intensity was observed after 2 hours compared to cells grown in the presence of glucose (Fig. S58). Subsequent addition of potassium cyanide (0.1 mM) resulted in a significant and rapid decrease in the observed emission intensity, with almost 85% of luminescence lost after 10 minutes (Figure 10). These results suggest that mitochondrial ATP is depleted substantially in the presence of KCN, due to inhibition of oxidative phosphorylation. ICP-MS analysis of cells incubated with [**Eu.3**]$^+$ for 30 minutes with KCN under glucose starvation conditions showed less than 10% variation in the concentration of accumulated Eu(III) metal, relative to untreated cells grown in the presence of glucose. Therefore, the possibility that incubation with KCN promotes efflux of [**Eu.3**]$^+$ from the cells can be ruled out. Taken together, these live-cell imaging experiments demonstrate that [**Eu.3**]$^+$ is capable of signalling changes in the concentration of ATP in the mitochondria, and could provide a versatile imaging tool for studying cell metabolism and other ATP-requiring processes within a targeted organelle, in real-time.

Conclusions

We have developed a discrete, water-soluble cationic Eu(III) complex for monitoring dynamic changes in the concentration of ATP within the mitochondria of living cells. A series of luminescent Eu(III) complexes, [**Eu.1–4**]$^+$, was synthesised that bind reversibly to nucleoside polyphosphate anions with differential affinities in buffered aqueous solution at physiological pH. The affinity of the Eu(III) complexes towards NPPs and the magnitude of the emission spectral response is tunable by making modifications to the ligand structure. Hydrogen bond donor groups were introduced into the quinoline chromophores of [**Eu.1**]$^+$ and [**Eu.3**]$^+$ to enhance selectivity towards ATP and ADP over monophosphate anions. Complex [**Eu.3**]$^+$, bearing two neutral amide donors, binds most strongly to ATP (log K_a = 5.8), forming a stable ternary complex that exhibits intense, long-lived Eu(III) luminescence. [**Eu.3**]$^+$ can discriminate effectively between ATP, ADP and AMP in a competitive aqueous medium that simulates the complex ionic environment present in cells. The probe provides a linear emission response that is proportional to the ratio of ATP/ADP, enabling the enzymatic hydrolysis of ATP to ADP to be precisely monitored in real-time.

Cellular localization studies revealed that [**Eu.3**]$^+$ preferentially stains the mitochondria of mammalian cells, and is retained within this organelle over extended time periods. We demonstrated that [**Eu.3**]$^+$ can detect an increase in mitochondrial ATP concentration following treatment of cells with the kinase inhibitor staurosporine. Additionally, [**Eu.3**]$^+$ was able to visualize a rapid decrease in mitochondrial ATP following treatment with KCN, an inhibitor of oxidative phosphorylation. Complex [**Eu.3**]$^+$ offers a several advances in performance compared to existing ATP-responsive probes, including a luminescence signal that is: 1) sensitive to ATP within the biologically relevant concentration range (1–5 mM); 2) minimally perturbed by changes in cellular pH or the presence of protein; and 3) sufficiently long-lived to avoid interference from UV-induced autofluorescence arising from biomolecules. Such probes offer a new versatile tool for studying cellular metabolism and a range of biological processes involving ATP. The strategy employed here will be explored further to design Eu(III) probes capable of monitoring spatio-temporal ATP dynamics within different cellular compartments, providing a ratiometric change in emission intensity that is intrinsically normalized.

Experimental Section

Comprehensive experimental details are provided in the supporting information, including: details of compound characterization, UV-Vis and emission spectral data for [**Eu.1–4**]$^+$, luminescence titration experiments involving [**Eu.1–4**]$^+$ and NPP anions (conducted in buffered aqueous solution and competitive aqueous media), pH dependence of the emission profile of [**Eu.3**]$^+$, ICP-MS data, cellular imaging analysis and selected LSCM images of [**Eu.3**]$^+$ in NIH-3T3 cells.

Acknowledgements

This work was supported by a Wellcome Trust Seed Award (204500/Z/16/Z) and a Royal Society of Chemistry Research Grant. SJB would like to thank Dr. David Worrall for use of fluorescence spectroscopy facilities and Dr. Matthew Turner for support with mass spectrometric analysis. RP would like to acknowledge the Royal Society URF.

Keywords: adenosine triphosphate (ATP) • live cell imaging • anion receptor • lanthanide • luminescence

References:

‡ Anion affinity constants for [**Eu.3**]$^+$ were determined by plotting the change in the ratio of the $\Delta J = 2/\Delta J = 0$ (605–630/575–580 nm) emission bands as a function of anion concentration.
§ Major ESI mass spectral signals were also obtained for the ternary adducts of [**Eu.4**]$^+$ bound to 1 molecule of ATP or GTP (Figures S47 and S48).

[1] M. Rajendran, E. Dane, J. Conley, M. Tantama, *Biol. Bull.* **2016**, *231*, 73–84.
[2] R. D. Fields, B. Stevens, *Trends Neurosci.* **2000**, *23*, 625–633.
[3] S. Seino, T. Miki, *Prog. Biophys.Mol. Biol.* **2003**, *81*,133–176.
[4] M. V. Zamaraeva, R. Z. Sabirov, E. Maeno, Y. Ando-Akatsuka, S. V. Bessonova, Y. Okada, *Cell Death Differ.* **2005**, *12*, 1390–1397.
[5] a) H. Imamura, K. P. Huynh Nhat, H. Togawa, K. Saito, R. Lino, Y. Kato-Yamada, T. Nagai, H. Noji. *Proc. Natl. Acad. Sci.* **2009**, *106*, 15651–15656; b) M. Tantama, J. R. Martínez-François, R. Mongeon, G. Yellen, *Nat. Commun.* **2013**, *4*, 2550–2550.
[6] a) S. E. Schneider, S. N. O'Neil, E. V. Anslyn, *J. Am. Chem. Soc.* **2000**, *122*, 542–543; b) A. Ojida, S.-k. Park, Y. Mito-oka and I. Hamachi, *Tetrahedron Lett.* **2002**, *43*, 6193–6195; c) K. M. K. Swamy, S. K. Kwon, H. N. Lee, S. M. S. Kumar, J. S. Kim and J. Yoon, *Tetrahedron Lett.* **2007**, *48*, 8683–8686; d) A. Sreenivasa Rao, D. Kim, H. Nam, H. Jo, K. H. Kim, C. Ban and K. H. Ahn, *Chem. Commun.* **2012**, *48*, 3206–3208; e) A. Ojida, I. Takashima, T. Kohira, H. Nonaka and I. Hamachi, *J. Am. Chem. Soc.* **2008**, *130*, 12095–12101; f) X. Liu, H. T. Ngo, Z. Ge, S. J. Butler and K. A. Jolliffe, *Chem. Sci.* **2013**, *4*, 1680–1686; g) X. Li, X. Guo, L. Cao, Z. Xun, S. Wang, S. Li, Y. Li and G. Yang, *Angew. Chem., Int. Ed.* **2014**, *53*, 7809–7813; h) Y. Zhou, Z. Xu and J. Yoon, *Chem. Soc. Rev.* **2011**, *40*, 2222–2235.
[7] a) Y. Kurishita, T. Kohira, A. Ojida and I. Hamachi, *J. Am. Chem. Soc.*, **2012**, *134*, 18779–18789; b) D. Maity, M. Li, M. Ehlers and C. Schmuck, *Chem. Commun.* **2017**, *53*, 208–211; c) L. Wang, L. Yuan, X. Zeng, J. Peng, Y. Ni, J. C. Er, W. Xu, B. K. Agrawalla, D. Su, B. Kim and Y.-T. Chang, *Angew. Chem., Int. Ed.* **2016**, *55*, 1773–1776; d) Z. Xu, N. J. Singh, J. Lim, J. Pan, H. N. Kim, S. Park, K. S. Kim and J. Yoon, *J. Am. Chem. Soc.* **2009**, *131*, 15528–15533.
[8] T. W. Traut, *Mol. Cell. Biochem.* **1994**, *140*, 1–22.
[9] a) M. C. Heffern, L. M. Matosziuk and T. J. Meade, *Chem. Rev.* **2014**, *114*, 4496–4539; b) E. J. New, D. Parker, D. G. Smith and J. W. Walton, *Curr. Opin. Chem. Biol.* **2010**, *14*, 238–246. c) M. P. Coogan and V. Fernandez-Moreira, *Chem. Commun.* **2014**, *50*, 384–399.
[10] J. W. Walton, A. Bourdolle, S. J. Butler, M. Soulie, M. Delbianco, B. K. McMahon, R. Pal, H. Puschmann, J. M. Zwier, L. Lamarque, O. Maury, C. Andraud and D. Parker, *Chem. Commun.*, **2013**, 49, 1600–1602.
[11] S. J. Butler, L. Lamarque, R. Pal and D. Parker, *Chem. Sci.* **2014**, *5*, 1750–1755.
[12] a) D. G. Smith, G. L. Law, B. S. Murray, R. Pal, D. Parker and K. L. Wong, *Chem. Commun.* **2011**, *47*, 7347–7349; b) S. J. Butler, B. K. McMahon, R. Pal, D. Parker and J. W. Walton, *Chem. - Eur. J.* **2013**, *19*, 9511–9517; c) D. G. Smith, R. Pal and D. Parker, *Chem. - Eur. J.* **2012**, *18*, 11604–11613.
[13] a) S. J. Butler, *Chem. Commun.* **2015**, *51*, 10879–10882; b) O. A. Blackburn, A. M. Kenwright, A. R. Jupp, J. M. Goicoechea, P. D. Beer and S. Faulkner, *Chem. - Eur. J.* **2016**, *22*, 8929–8936; c) T. Liu, A. Nonat, M. Beyler, M. Regueiro-Figueroa, K. Nchimi Nono, O. Jeannin, F. Camerel, F. Debaene, S. Cianferani-Sanglier, R. Tripier, C. Platas-Iglesias and L. J. Charbonniere, *Angew. Chem., Int. Ed.* **2014**, *53*, 7259–7263.
[14] a) L. J. Charbonnière, R. Schurhammer, S. Mameri, G. Wipff and R. F. Ziessel, *Inorg. Chem.* **2005**, *44*, 7151–7160; b) S. Nadella, J. Sahoo, P. S. Subramanian, A. Sahu, S. Mishra and M. Albrecht, *Chem. - Eur. J.* **2014**, *20*, 6047–6053; c) D. F. Caffrey and T. Gunnlaugsson, *Dalton Trans.* **2014**, *43*, 17964–17970.
[15] a) R. Pal, D. Parker and L. C. Costello, *Org. Biomol. Chem.* **2009**, *7*, 1525–1528; b) R. S. Dickins, S. Aime, A. S. Batsanov, A. Beeby, M. Botta, J. I. Bruce, J. A. K. Howard, C. S. Love, D. Parker, R. D. Peacock and H. Puschmann, *J. Am. Chem. Soc.* **2002**, *124*, 12697–12705.
[16] a) S. H. Hewitt, R. Liu, S. J. Butler, *Supramol. Chem.* **2017**, DOI. 10.1080/10610278.2017.1410548; b) P. Atkinson, B. S. Murray, D. Parker, *Org. Biomol. Chem.* **2006,** *4*, 3166–3171; c) K. L. Gempf, S. J. Butler, A. M. Funk, D. Parker, *Chem. Commun.*, **2013,** *49*, 9104-6.
[17] S. J. Butler, D. Parker, *Chem. Soc. Rev.* **2013**, *42*, 1652–1666.
[18] A. B. Aletti, D. M. Gillen, T. Gunnlaugsson, *Coord. Chem. Rev.* **2018**, *354*, 98–120.
[19] E. A. Weitz, J. Y. Chang, A. H. Rosenfield and V. C. Pierre, *J. Am. Chem. Soc.* **2012**, *134*, 16099–16102.
[20] M. Schäferling, T. Ääritalo and T. Soukka, *Chem. - Eur. J.* **2014**, *20*, 5298–5308.
[21] E. A. Weitz, J. Y. Chang, A. H. Rosenfield, E. A. Morrow and V. C. Pierre, *Chem. Sci.* **2013**, *4*, 4052–4060.
[22] M. Schaferling and O. S. Wolfbeis, *Chem. - Eur. J.* **2007**, *13*, 4342–4349.
[23] X. Liu, J. Xu, Y. Lv, W. Wu, W. Liu and Y. Tang, *Dalton Trans.* **2013**, *42*, 9840–9846.
[24] S. H. Hewitt, J. Parris, R. Mailhot and S. J. Butler, *Chem. Commun.* **2017**, *53*, 12626–12629.
[25] S. J. Butler, *Chem. - Eur. J.* **2014**, *20*, 15768–15774.
[26] A. Beeby, I. M. Clarkson, R. S. Dickins, S. Faulkner, D. Parker, L. Royle, A. S. de Sousa, J. A. Gareth Williams and M. Woods, *J. Chem. Soc., Perkin Trans. 2.* **1999**, *0*, 493–504.
[27] E. Gout, F. Rébeillé, R. Douce and R. Bligny, *Proc. Natl. Acad. Sci.* **2014**, *111*, E4560-E4567.
[28] L. Yu, L. Xu, M. Xu, B. Wan, L. Yu and Q. Huang, *Mol. Simul.* **2011**, *37*, 1143–1150.
[29] a) C. T. Burt, H. M. Cheng, S. Gabel and R. E. London, *J. Biochem.* **1990**, *108*, 441–448; b) G. D. Williams, T. J. Mosher and M. B. Smith, *Anal. Biochem.* **1993**, *214*, 458–467; c) V. L. Pecoraro, J. D. Hermes and W. W. Cleland, *Biochemistry,* **1984**, *23*, 5262–5271.
[30] Y. Kurishita, T. Kohira, A. Ojida and I. Hamachi, *J. Am. Chem. Soc.* **2010**, *132*, 13290–13299.
[31] For examples of enzyme assays involving reactions with emissive Ln(III) complexes see: a) B. K. McMahon and T. Gunnlaugsson, *J. Am. Chem. Soc.*, **2012**, *134*, 10725–10728; b) H. M. Burke, T. Gunnlaugsson and E. M. Scanlan, *Org. Biomol. Chem.*, **2016**, *14*, 9133–9145.
[32] a) S. H. Hewitt and A. J. Wilson, *Chem. Commun.* **2016**, *52*, 9745–9756; b) V. Fernandez-Moreira, F. L. Thorp-Greenwood and M. P. Coogan, *Chem. Commun.* **2010**, *46*, 186–202.
[33] B. Xiao, M. J. Sanders, E. Underwood, R. Heath, F. V. Mayer, D. Carmena, C. Jing, P. A. Walker, J. F. Eccleston, L. F. Haire, P. Saiu, S. A. Howell, R. Aasland, S. R. Martin, D. Carling and S. J. Gamblin, *Nature*, **2011**, *472*, 230–233.
[34] J. Llopis, J. M. McCaffery, A. Miyawaki, M. G. Farquhar and R. Y. Tsien, *Proc. Natl. Acad. Sci.* **1998**, *95*, 6803–6808.
[35] R. Pal, *Faraday Discussions*, **2015**, *177*, 507–515.

FULL PAPER

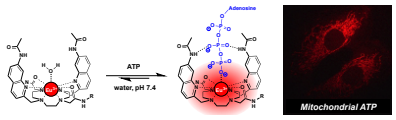

We report a short series of cationic Eu(III) complexes for monitoring dynamic changes in the concentration of ATP within the mitochondria of living cells. Complex [**Eu.3**]$^{+}$ binds reversibly to ATP and responds linearly to this anion within the physiological range (1–5 mM). The probe was used to visualize elevated ATP levels following treatment with a broad spectrum kinase inhibitor, staurosporine, as well as depleted ATP levels upon treatment with KCN under glucose starvation conditions.

*Romain Mailhot, Thomas Traviss-Pollard, Robert Pal and Stephen J. Butler**

Page No. – Page No.

Cationic Europium Complexes for Visualizing Fluctuations in Mitochondrial ATP Levels in Living Cells